© 2017. Published by The Company of Biologists Ltd | Journal of Experimental Biology (2017) 220, 1400-1404 doi:10.1242/jeb.154583

SHORT COMMUNICATION

Caspase-3 and GFAP as early markers for apoptosis and astrogliosis in shRNA-induced hippocampal cytotoxicity

Anne Günther[1,*], Vince Luczak[2], Ted Abel[2] and Arnd Baumann[1,‡]

ABSTRACT

Genetic manipulation of cells and tissue by RNA interference has significantly contributed to the functional characterization of individual proteins and their role in physiological processes. Despite its versatility, RNA interference can have detrimental side effects, including reduced cell viability. We applied recombinant adeno-associated viruses by stereotaxic injection into the murine hippocampus to express different short hairpin RNA (shRNA) constructs along with eGFP. Tissue responses were assessed immunohistochemically for up to 8 weeks post-infection. Strong hippocampal degeneration and tissue atrophy was observed, most likely induced by high shRNA expression. The effect was entirely absent in mice injected with vectors driving only expression of eGFP. Active caspase-3 (Casp-3) and glial fibrillary acidic protein (GFAP) were identified as molecular markers and early indicators of adverse tissue responses. Our findings also demonstrate that detrimental effects of high shRNA expression in hippocampal tissue can be monitored even before the onset of tissue degeneration.

KEY WORDS: RNAi, Neurotoxicity, Hippocampus, Adeno-associated virus, Tissue atrophy

INTRODUCTION

RNA interference (RNAi) is a popular technique for uncovering the function of individual proteins in cells or organisms (Shan, 2010). As short hairpin RNAs (shRNAs) can be designed specifically for any structural gene, they provide an extensive toolbox for RNAi-based manipulation of gene expression. However, some adverse effects of shRNA expression, including reduced cell viability, have been observed (Ehlert et al., 2010; Grimm et al., 2006).

Certain aspects of shRNA-induced cytotoxicity have been described in previous studies (Börner et al., 2013; Bridge et al., 2003; Grimm et al., 2010; Sledz et al., 2003; Yi et al., 2005). Notably, shRNA-induced neurotoxicity is affected by various factors, such as shRNA sequence, shRNA concentration applied, means of application (e.g. virus-mediated delivery and expression), as well as the treated brain region. Whereas shRNA-induced neurotoxicity culminating in tissue atrophy has been described for some CNS regions, including the striatum (Martin et al., 2011; McBride et al., 2008), adverse effects have not yet been described in the mouse hippocampus. Nonetheless, virus-mediated delivery of shRNA-expressing constructs is used increasingly to investigate the contribution of individual proteins to hippocampal function on the cellular and subcellular level. At present, information on molecular markers for shRNA-induced tissue stress, even before apparent tissue degeneration, is scarce. Testing for the expression of such markers would allow assessment of any treatment-induced side effects in behavioral studies using shRNA-based approaches.

Here, we report on shRNA-induced degeneration in the murine hippocampus. We examined tissue sections after rAAV9-mediated expression of shRNA constructs by immunohistochemistry. In samples with high expression of different shRNA constructs, strong degeneration and tissue atrophy were detected. We identified two markers, active caspase-3 (Casp-3) and glial fibrillary acidic protein (GFAP), that indicate adverse side effects of shRNA treatment even before tissue degeneration could be observed.

MATERIALS AND METHODS

Vector generation

Sequences encoding the human U6 (hU6) promoter and shRNA constructs directed against two hyperpolarization-activated and cyclic nucleotide-gated channel genes, *hcn1* (CCG GCC TCC AAT CAA CTA TCC TCA ACT CGA GTT GAG GAT AGT TGA TTG GAG GTT TTT G, no. TRCN0000103027) and *hcn2* (CCG GCC ATG CTG ACA AAG CTC AAA TCT CGA GAT TTG AGC TTT GTC AGC ATG GTT TTT G, no. TRCN0000103001), were purchased from Sigma-Aldrich (Munich, Germany). A construct encoding a *Photinus pyralis* luciferase (*luc*)-targeting shRNA sequence (Premsrirut et al., 2011) was designed (CCG GCC GCC TGA AGT CTC TGA TTA ACT CGA GTT AAT CAG AGA CTT CAG GCG GTT TTT G) and synthesized (MWG Operon, Ebersberg, Germany). Constructs were cloned into the rAAV vector pENN-CaMKIIeGFP provided by the University of Pennsylvania Vector Core (see Fig. 1). Viral particles were packaged by the University of Pennsylvania Vector Core and genomic titers ranged from 10^9 to 10^{10} genome copies μl^{-1}.

Animals and stereotaxic injection

A total of 10 male C57BL/6J mice (The Jackson Laboratory, Bar Harbor, ME, USA) were used in this study for viral injection and subsequent immunohistochemical analysis. Animals were housed in groups of 4–5 under standard conditions with access to food and water *ad libitum* on a 12 h:12 h light:dark cycle. Experiments were carried out in accordance with National Institutes of Health guidelines and were approved by the University of Pennsylvania Institutional Animal Care and Use Committee. Mice received bilateral intra-hippocampal injections of rAAV9 vectors encoding enhanced green fluorescent protein (eGFP) and shRNA constructs at 8–10 weeks of age. Stereotaxic injection of 1 µl viral suspension (0.2 µl min^{-1}) per hippocampus was performed at antero-posterior −1.9, medio-lateral ±1.5 and dorso-ventral −1.4 from Bregma using

[1]Institute of Complex Systems, Cellular Biophysics (ICS-4), Forschungszentrum Jülich, Jülich 52425, Germany. [2]Department of Biology, University of Pennsylvania, Philadelphia, PA 19104, USA.
*Present address: (A.G.) RIKEN Brain Science Institute, Synaptic Molecules of Memory Persistence, Wako, Saitama 351-0198, Japan

‡Author for correspondence (a.baumann@fz-juelich.de)

A.B., 0000-0001-9456-7275

Received 12 December 2016; Accepted 1 February 2017

Journal of Experimental Biology

Journal of Experimental Biology (2017) 220, 1400-1404 doi:10.1242/jeb.154583

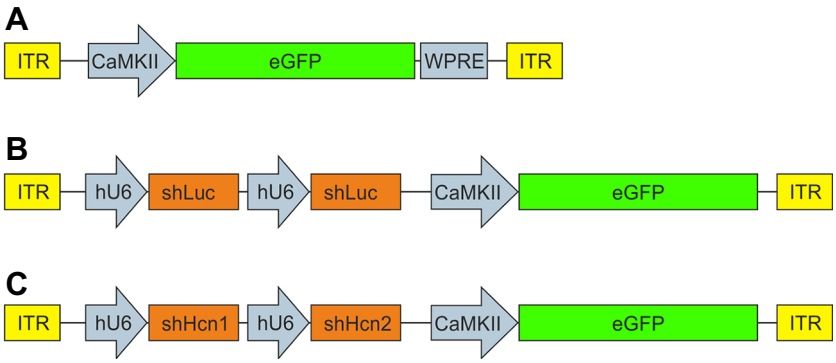

Fig. 1. Schematic representation of adeno-associated viral vector constructs. Viral vectors were designed to encode enhanced green fluorescent protein (eGFP) under the control of the neuron-specific CaMKIIα promoter and two short hairpin RNA (shRNA) sequences under the control of the human U6 (hU6) promoter. The shRNA expression cassettes were placed upstream of the eGFP expression cassette. The constructs were flanked by inverted terminal repeats (ITR) for viral packaging. (A) The control construct encoding only eGFP with the woodchuck hepatitis virus post-transcriptional regulatory element (WPRE). (B) The *luc*-targeting construct. (C) The *hcn*-targeting construct. Sequence segments are indicated by colored bars.

a 33 gauge beveled NanoFil needle, a NanoFil syringe and a MicroSyringe Pump Controller (World Precision Instruments, Sarasota, FL, USA). After surgery, mice were single-housed and given 5 days to recover before pair-housing. Injection and tissue collection were performed during the light phase.

Primary hippocampal neurons

Hippocampal tissue from 1–3-day-old mice (C57BL/6 strain from an in-house animal breeding facility) was prepared in ice-cold HBSS (Hanks' balanced salt solution). Hippocampi were incubated in papain solution [DMEM (Invitrogen), 25 U ml^{-1} papain, 1.6 mmol l^{-1} L-cysteine, 1 mmol l^{-1} $CaCl_2$, 0.5 mmol l^{-1} EDTA] at 37°C for 20 min and subsequently in inactivating solution [2.5% (w/v) trypsin inhibitor, 2.5% (w/v) albumin, in FCS solution] at 37°C for 5 min. Cells were triturated in FCS solution [DMEM, 100 U ml^{-1}:100 µg ml^{-1} streptomycin:penicillin, 10% FCS, 0.1% (v/v) MITO+ serum extender]. Primary hippocampal neurons (PHNs) were plated on µ-Slide 4 Well slides (Ibidi, Martinsried, Germany) pre-coated with poly-D-lysine (0.2 mg ml^{-1} poly-D-lysine, 50 mmol l^{-1} H_3BO_3, 25 mmol l^{-1} $Na_2B_4O_7$, pH 8.5). PHNs were maintained in NBA medium [Neurobasal A Medium (Invitrogen), 100 U ml^{-1}:100 µg ml^{-1} streptomycin:penicillin, 2% (v/v) B27-supplement (Invitrogen) and 1% (v/v) Glutamax] at 37°C, 5% CO_2 and 95% relative humidity for 14 days.

Quantification of gene expression by real-time PCR

Total RNA was isolated from PHN cultures using the DNA/RNA/Protein AllPrep® Kit (Qiagen, Hilden, Germany) according to the supplier's protocol. RNA samples were split for two independent first-strand cDNA syntheses using Oligo-dT primers (Qiagen) and Moloney Murine Leukemia Virus reverse transcriptase (M-MLV-RT, Life Technologies) according to the supplier's protocol. Thermocycling was performed in a LightCycler 1.5 (Roche, Mannheim, Germany) using the QuantiTect SYBR Green PCR Kit (Qiagen) according to the supplier's protocol. Gene-specific primers (Table S1) were designed *in silico* and synthesized by MWG Operon (Ebersberg, Germany). Specificity and efficiency of primers was confirmed via BLAST analysis and semi-quantitative PCR on cloned gene fragments (Figs S1, S2). The *gapdh* primers were designed to bind in exons separated by an intron of 134 bp to check for genomic impurities.

qPCR reactions were performed on 1 µl aliquots of first-strand cDNA samples in a total volume of 20 µl. Results were analyzed using the Ct method. Gene expression levels were normalized to expression of the housekeeping gene *gapdh*. For analysis, mean± s.e.m. values were calculated. The two-tailed independent Student's *t*-test was applied for calculation of *P*-values. A *P*-value of <0.05 was considered significant.

Antibodies and immunohistochemistry

For immunohistochemical analysis, brains were dissected after transcardial perfusion with ice-cold PBS followed by 4% paraformaldehyde in PBS under deep anesthesia. Tissues were cryo-protected in 30% sucrose (in PBS) for 2 days, embedded in Tissue Tek (Sakura Finetek, Zouterwoude, The Netherlands), and coronal cryo-sections (30 µm) were prepared.

For immunohistochemical staining, sections were incubated in 0.3% (v/v) H_2O_2 for 30 min at room temperature before unspecific binding sites were blocked for 1 h at room temperature in blocking solution [0.75% (v/v) Triton X-100, 5% (v/v) normal goat serum (NGS), 5% (v/v) normal donkey serum (NDS), in PBS]. Subsequently, slices were incubated at 4°C for 3 days with primary antibodies (active Casp-3, 1:50, ab2302, Abcam, Milton, UK; GFAP, 1:500, MAB3402, Millipore, Hohenbrunn, Germany) diluted in incubating solution [0.75% (v/v) Triton X-100, 0.5% (v/v) NGS, 0.5% (v/v) NDS, in PBS]. After washing with PBS, samples were incubated at room temperature for 4 h with secondary antibodies (gt-α-msA647, 1:50, A-21235, Life Technologies, Carlsbad, CA, USA; gt-α-rbA555, 1:500, A-21428, Life Technologies) diluted in incubating solution. For DAPI staining, NucBlue Reagent (Life Technologies) was used according to the supplier's protocol. Slices were washed, transferred onto slides (SuperFrost Plus, Menzel, Braunschweig, Germany) and, finally, a coverslip was fixed on the samples with Aqua-Poly/Mount (Polysciences, Eppelheim, Germany). Fluorescent images were obtained with an inverted confocal microscope (TCS SP8, Leica, Wetzlar, Germany).

RESULTS AND DISCUSSION

We applied recombinant adeno-associated virus serotype 9 (rAAV9) vectors for injection into the murine hippocampus. Viral vectors were designed to mediate expression of shRNA constructs targeting independent genes, i.e. *hcn* and *luc*. Because of their low immunogenicity, rAAV vectors are generally considered to be an optimal tool for genetic manipulation *in vivo*.

We designed viral constructs to express two distinct shRNA-encoding fragments as well as eGFP for the identification of infected cells (Fig. 1). Prior to stereotaxic injection, viral constructs were tested for knockdown efficiency and specificity of endogenous *hcn1* and *hcn2* expression in primary hippocampal neurons by qPCR. We assessed cell viability and morphology in primary cultures by immunofluorescence microscopy of neurons co-expressing shRNA and eGFP in comparison either to neurons transduced with rAAV vectors mediating only eGFP expression or to non-transduced control cultures. No detrimental effects on the health of neurons were observed in these cultures (data not shown).

Journal of Experimental Biology (2017) 220, 1400-1404 doi:10.1242/jeb.154583

After establishing the functionality of shRNAs *in vitro*, rAAV9 vectors were injected into the dorsal hippocampus. Animals were killed at 3–8 weeks post-infection. We observed widespread eGFP fluorescence in hippocampal tissue after a single stereotaxic injection of rAAV9 constructs (Fig. 2). Expression of eGFP was driven by the neuron-specific CaMKIIα promoter, whereas shRNAs were expressed under the control of the constitutive hU6 promoter. Because of vector design, transduced neurons can be identified on the basis of eGFP fluorescence, whereas transduced non-neuronal cells do not show eGFP fluorescence, but could still express shRNAs.

Some animals injected with shRNA-encoding rAAVs displayed neuronal degeneration at 3 weeks post-infection (Fig. 2D). In contrast, eGFP expression alone did not induce an adverse tissue response (Fig. 2B), confirming that the degeneration was not due to eGFP expression *per se*. Tissue degeneration advanced with time and was even stronger in animals injected with *luc*-targeting control constructs than with *hcn*-targeting constructs.

In order to further assess the observed tissue degeneration, we examined the expression of potential cellular stress markers (Fig. 3), including Casp-3 and GFAP. As all of the applied rAAV constructs encoded eGFP as a marker, transduction of the dorsal hippocampus was monitored based on eGFP fluorescence. Strong immunoreactivity of Casp-3 and GFAP was observed in the dorsal hippocampus at 3 weeks post-infection even though tissue degeneration was not yet apparent. Neither Casp-3 nor GFAP was detected in the ventral hippocampus at this time point. At 4 weeks post-infection, degeneration in the dorsal hippocampus became apparent and immunoreactivity of Casp-3 and GFAP was also detected in more ventral regions of the hippocampal formation. Notably, detection of Casp-3 and GFAP was always in concordance with eGFP expression.

RNAi-based strategies frequently use viral vectors for specific manipulation of gene expression at defined tissue sites in the rodent brain. Previous studies have employed shRNA constructs without apparent detrimental effects on cell viability in the hippocampus (Mosser et al., 2015; Omata et al., 2011; Kim et al., 2012). In this study, we applied virus titers within the range chosen by most rAAV-based RNAi studies in the CNS, i.e. between 10^9 and 10^{11} total virus particles. We examined three different eGFP-encoding rAAV9 constructs. Viral vectors mediated expression of:

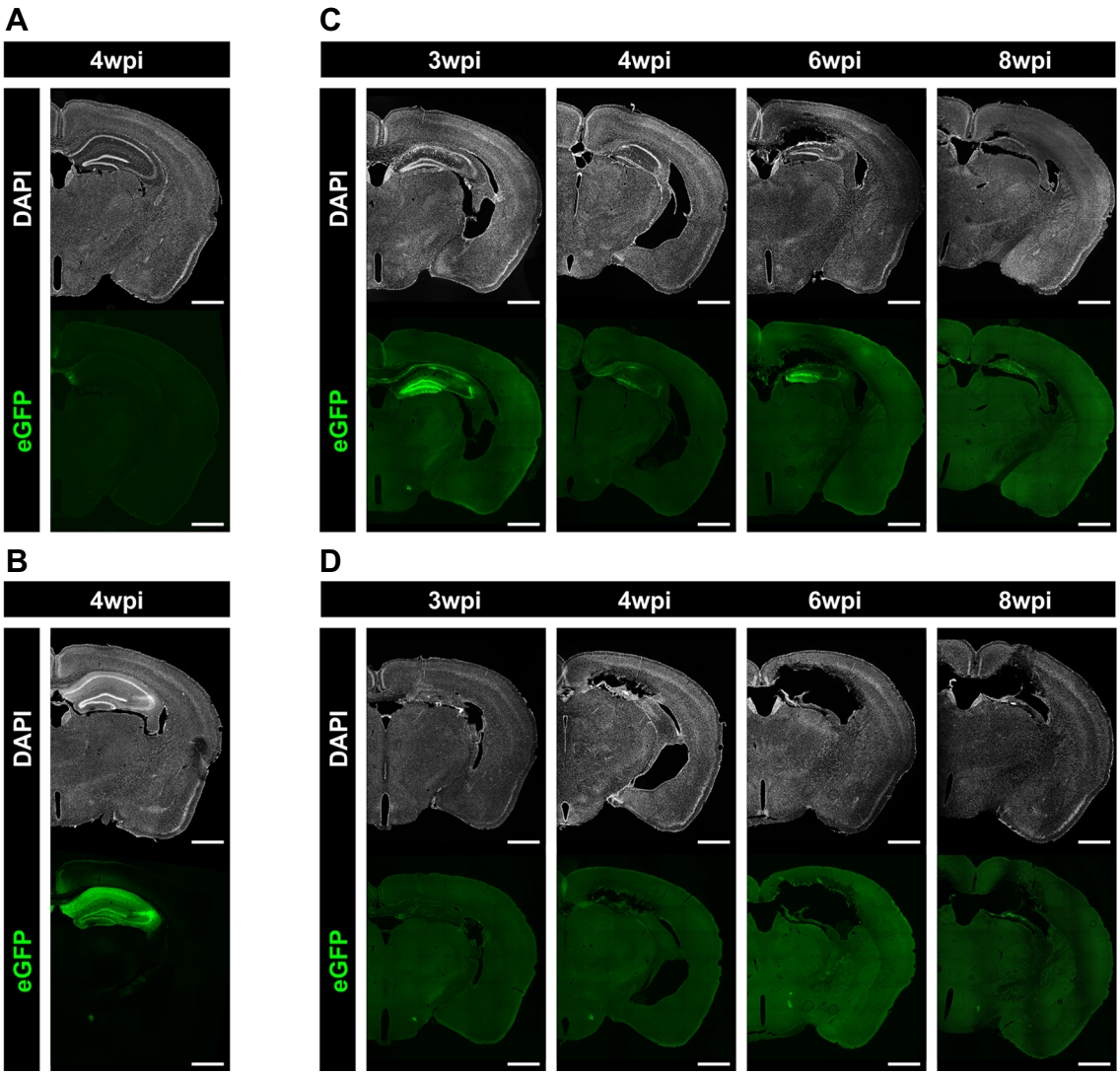

Fig. 2. Injection of rAAV9 vectors in the hippocampus. Immunohistochemical analysis of coronal sections at different time points after injection. Sections of the dorsal hippocampus are shown, depicting eGFP fluorescence in green and DAPI staining of nuclei in gray. Injection of different rAAV9 constructs is as follows: (A) non-injected, (B) eGFP-encoding construct, (C) *hcn*-targeting shRNA and (D) *luc*-targeting shRNA. Time points are indicated above the images as weeks post-infection (wpi). Scale bars, 1 mm.

Journal of Experimental Biology

Journal of Experimental Biology (2017) 220, 1400-1404 doi:10.1242/jeb.154583

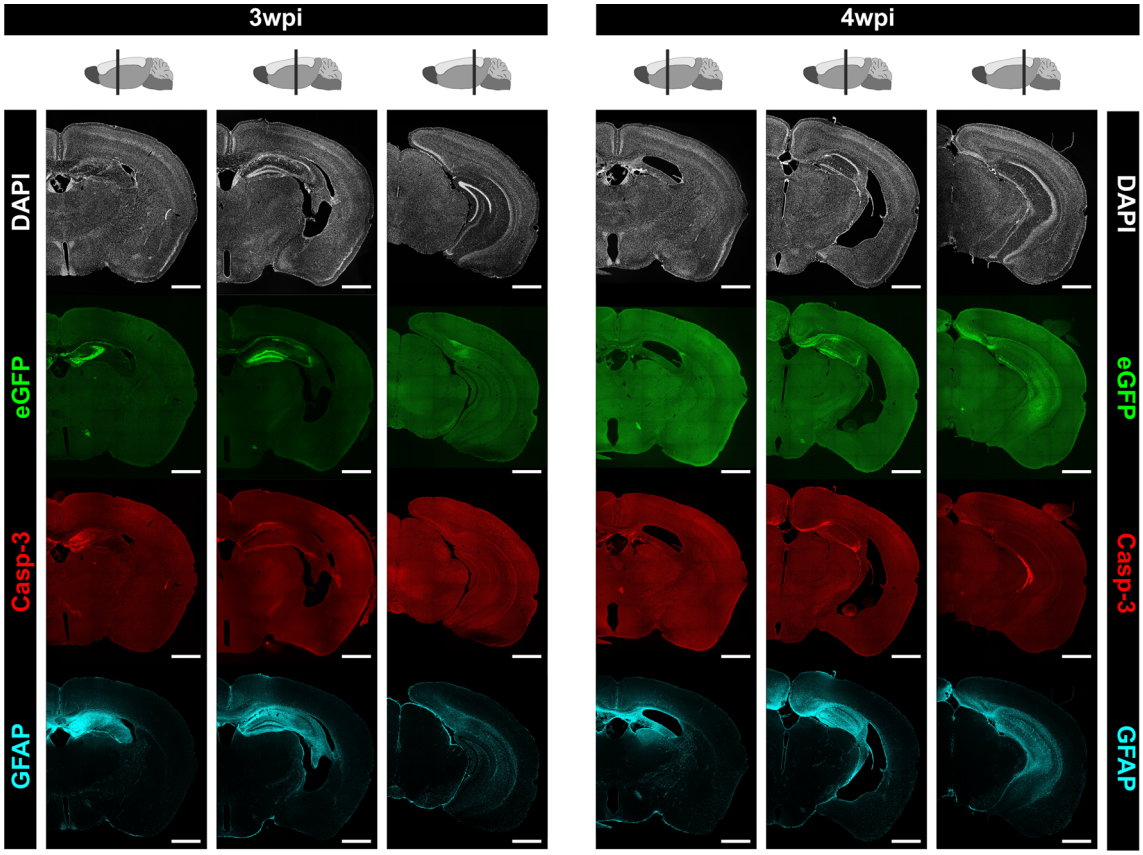

Fig. 3. Markers of shRNA-induced tissue degeneration in the hippocampus. Mice were injected with rAAV9 encoding *hcn*-targeting shRNA sequences. Immunohistochemical analysis of animals was carried out at 3 and 4 weeks post-infection. Positions of sections along the antero-posterior axis of the brain are indicated schematically. DAPI staining of nuclei is depicted in gray, eGFP fluorescence in green, caspase-3 (Casp-3) staining in red and glial fibrillary acidic protein (GFAP) staining in cyan. Proteins were stained with specific antibodies and examined by confocal microscopy. *Z*-stacks (5×3 µm sections) were registered and average intensity projections were generated. Scale bars, 1 mm.

(1) shRNAs targeting endogenous *hcn* genes, (2) shRNAs targeting the *luc* gene, which is not endogenously expressed in mammals and is used widely as a control in similar studies, and (3) a negative control without a shRNA-encoding sequence. Surprisingly, even though no adverse effects of the shRNA-encoding constructs were observed in primary hippocampal neurons cultivated *in vitro*, rAAV9-mediated shRNA expression induced strong cellular degeneration in the hippocampus of mice (see Fig. 2). The detrimental effects were independent of the encoded shRNA sequence as they were observed for constructs targeting both endogenous and non-endogenous transcripts (i.e. *hcn* and *luc*), but were not apparent in animals treated with rAAVs encoding only eGFP.

Cytotoxic effects of shRNAs have previously been shown to be caused by overloading of the endogenous miRNA machinery (Börner et al., 2013; Grimm et al., 2006, 2010; McBride et al., 2008; Yi et al., 2005). These observations were corroborated by the pronounced shRNA dose dependency of cytotoxicity (Grimm, 2011). However, as the total number of virus particles may vary depending on the applied construct and the treated CNS region, potential effects on the tissue must be assessed for each construct, individually. As AAV9 is known to transduce neurons as well as astrocytes (Aschauer et al., 2013), we cannot rule out that constitutive shRNA expression in astrocytes might be an additional factor in the observed hippocampal degeneration.

So far, reports examining shRNA-induced cytotoxicity have not consistently described the expression of molecular markers related to tissue degeneration (Bauer et al., 2009; Hutson et al., 2014; Martin et al., 2011; McBride et al., 2008). To address this issue in the context of the observed hippocampal degeneration, we assessed expression of Casp-3, a marker of apoptosis (Ashkenazi and Salvesen, 2014), and GFAP, a marker of astroglial activation (Sofroniew, 2009). Expression of both molecular markers strongly correlated with rAAV9-mediated shRNA expression.

Our results emphasize that detrimental effects of shRNA application *in vivo* might not always be readily identified in cell culture. We suggest that the design of shRNA-based studies should involve careful consideration of several parameters, such as shRNA dose (Grimm, 2011), promoter choice (Lebbink et al., 2011; Sun et al., 2013), AAV serotype (Ehlert et al., 2010) and construct backbone (Boudreau et al., 2009; Han et al., 2011; McBride et al., 2008). These factors should subsequently be tested with respect to titer, construct and specificity *in vivo*. Furthermore, RNAi-based studies should take into account that the detrimental effects observed here for standard C57BL/6J mice may differ depending on the employed mouse strains. However, the identification of reliable markers, such as increased Casp-3 and GFAP expression, for monitoring shRNA-induced tissue stress even before the onset of degeneration is a requirement for validating behavioral experiments that are based on RNAi strategies.

Acknowledgements

We gratefully acknowledge the assistance of Dr H. Büning with establishing the rAAV cell culture. We thank Dr D. Kaschuba for her help with the identification of *hcn*-targeting shRNA constructs.

Competing interests
The authors declare no competing or financial interests.

Author contributions
A.G., A.B. and T.A. designed the study. A.G. planned and cloned the rAAVs. A.G. and V.L. performed AAV injection. A.G. performed the immunological analysis. A.G. wrote the manuscript. A.G., A.B. and T.A. revised the manuscript.

Funding
This work was supported by the National Institutes of Health (grant RO1 MH 099544 to PI: T.A.) and the National Science Foundation (grant 1515458 to PI: T.A.). Deposited in PMC for release after 12 months.

Supplementary information
Supplementary information available online at
http://jeb.biologists.org/lookup/doi/10.1242/jeb.154583.supplemental

References
Aschauer, D. F., Kreuz, S. and Rumpel, S. (2013). Analysis of transduction efficiency, tropism and axonal transport of AAV serotypes 1, 2, 5, 6, 8 and 9 in the mouse brain. *PLoS ONE* **8**, e76310.

Ashkenazi, A. and Salvesen, G. (2014). Regulated cell death: signaling and mechanisms. *Annu. Rev. Cell Dev. Biol.* **30**, 337-356.

Bauer, M., Kinkl, N., Meixner, A., Kremmer, E., Riemenschneider, M., Förstl, H., Gasser, T. and Ueffing, M. (2009). Prevention of interferon-stimulated gene expression using microRNA-designed hairpins. *Gene Ther.* **16**, 142-147.

Börner, K., Niopek, D., Cotugno, G., Kaldenbach, M., Pankert, T., Willemsen, J., Zhang, X., Schürmann, N., Mockenhaupt, S., Serva, A. et al. (2013). Robust RNAi enhancement via human Argonaute-2 overexpression from plasmids, viral vectors and cell lines. *Nucleic Acids Res.* **41**, e199.

Boudreau, R. L., Martins, I. and Davidson, B. L. (2009). Artificial microRNAs as siRNA shuttles: improved safety as compared to shRNAs *in vitro* and *in vivo*. *Mol. Ther. J. Am. Soc. Gene Ther.* **17**, 169-175.

Bridge, A. J., Pebernard, S., Ducraux, A., Nicoulaz, A.-L. and Iggo, R. (2003). Induction of an interferon response by RNAi vectors in mammalian cells. *Nat. Genet.* **34**, 263-264.

Ehlert, E. M., Eggers, R., Niclou, S. P. and Verhaagen, J. (2010). Cellular toxicity following application of adeno-associated viral vector-mediated RNA interference in the nervous system. *BMC Neurosci.* **11**, 20.

Grimm, D. (2011). The dose can make the poison: lessons learned from adverse in vivo toxicities caused by RNAi overexpression. *Silence* **2**, 8.

Grimm, D., Streetz, K. L., Jopling, C. L., Storm, T. A., Pandey, K., Davis, C. R., Marion, P., Salazar, F. and Kay, M. A. (2006). Fatality in mice due to oversaturation of cellular microRNA/short hairpin RNA pathways. *Nature* **441**, 537-541.

Grimm, D., Wang, L., Lee, J. S., Schürmann, N., Gu, S., Börner, K., Storm, T. A. and Kay, M. A. (2010). Argonaute proteins are key determinants of RNAi efficacy, toxicity, and persistence in the adult mouse liver. *J. Clin. Invest.* **120**, 3106-3119.

Han, Y., Khodr, C. E., Sapru, M. K., Pedapati, J. and Bohn, M. C. (2011). A microRNA embedded AAV α-synuclein gene silencing vector for dopaminergic neurons. *Brain Res.* **1386**, 15-24.

Hutson, T. H., Foster, E., Moon, L. D. F. and Yáñez-Muñoz, R. J. (2014). Lentiviral vector-mediated RNA silencing in the central nervous system. *Hum. Gene Ther. Methods* **25**, 14-32.

Kim, C. S., Chang, P. Y. and Johnston, D. (2012). Enhancement of dorsal hippocampal activity by knockdown of HCN1 channels leads to anxiolytic- and antidepressant-like behaviors. *Neuron* **75**, 503-516.

Lebbink, R. J., Lowe, M., Chan, T., Khine, H., Wang, X. and McManus, M. T. (2011). Polymerase II promoter strength determines efficacy of microRNA adapted shRNAs. *PLoS ONE* **6**, e26213.

Martin, J. N., Wolken, N., Brown, T., Dauer, W. T., Ehrlich, M. E. and Gonzalez-Alegre, P. (2011). Lethal toxicity caused by expression of shRNA in the mouse striatum: implications for therapeutic design. *Gene Ther.* **18**, 666-673.

McBride, J. L., Boudreau, R. L., Harper, S. Q., Staber, P. D., Monteys, A. M., Martins, I., Gilmore, B. L., Burstein, H., Peluso, R. W., Polisky, B. et al. (2008). Artificial miRNAs mitigate shRNA-mediated toxicity in the brain: implications for the therapeutic development of RNAi. *Proc. Natl. Acad. Sci. USA* **105**, 5868-5873.

Mosser, S., Alattia, J.-R., Dimitrov, M., Matz, A., Pascual, J., Schneider, B. L. and Fraering, P. C. (2015). The adipocyte differentiation protein APMAP is an endogenous suppressor of Aβ production in the brain. *Hum. Mol. Genet.* **24**, 371-382.

Omata, N., Chiu, C.-T., Moya, P. R., Leng, Y., Wang, Z., Hunsberger, J. G., Leeds, P. and Chuang, D.-M. (2011). Lentivirally mediated GSK-3β silencing in the hippocampal dentate gyrus induces antidepressant-like effects in stressed mice. *Int. J. Neuropsychopharmacol.* **14**, 711-717.

Premsrirut, P. K., Dow, L. E., Kim, S. Y., Camiolo, M., Malone, C. D., Miething, C., Scuoppo, C., Zuber, J., Dickins, R. A., Kogan, S. C. et al. (2011). A rapid and scalable system for studying gene function in mice using conditional RNA interference. *Cell* **145**, 145-158.

Shan, G. (2010). RNA interference as a gene knockdown technique. *Int. J. Biochem. Cell Biol.* **42**, 1243-1251.

Sledz, C. A., Holko, M., de Veer, M. J., Silverman, R. H. and Williams, B. R. G. (2003). Activation of the interferon system by short-interfering RNAs. *Nat. Cell Biol.* **5**, 834-839.

Sofroniew, M. V. (2009). Molecular dissection of reactive astrogliosis and glial scar formation. *Trends Neurosci.* **32**, 638-647.

Sun, C.-P., Wu, T.-H., Chen, C.-C., Wu, P.-Y., Shih, Y.-M., Tsuneyama, K. and Tao, M.-H. (2013). Studies of efficacy and liver toxicity related to adeno-associated virus-mediated RNA interference. *Hum. Gene Ther.* **24**, 739-750.

Yi, R., Doehle, B. P., Qin, Y., Macara, I. G. and Cullen, B. R. (2005). Overexpression of exportin 5 enhances RNA interference mediated by short hairpin RNAs and microRNAs. *RNA* **11**, 220-226.

Table S1 Primer pairs for qPCR on cDNA from primary hippocampal neurons and mouse brain.

Primer sequences and amplicon sizes are based on mouse sequences (accession numbers: NM_008084.2 (*gapdh*), NM_010408.3 (*hcn1*), NM_008226.2 (*hcn2*)). Amplicon sizes of *gapdh* fragments are indicated for cDNA (150bp) and genomic DNA (284bp).

protein	gene	primer	sequence (5‘ →3‘)	T_m	amplicon size
GAPDH	*gapdh*	forward	GGTATCGTGGAAGGACTCATG	62°C	150bp/284bp
		reverse	GCTGCCAAGGCTGTGGGC		
HCN1	*hcn1*	forward	ACTGTGGGCGAATCCCTGG	62°C	184bp
		reverse	CCACCAGCAGCTGTGCAGA		
HCN2	*hcn2*	forward	GGAGAATGCCATCATCCAGG	62°C	149bp
		reverse	CAGCAGGCTGTGGCCATGA		

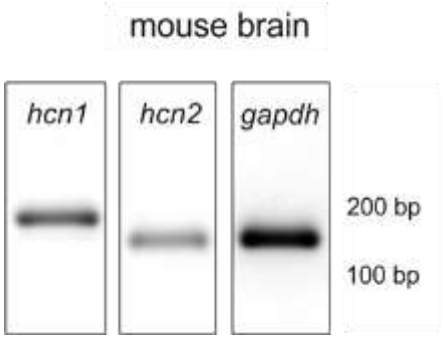

Fig. S1 Semi-quantitative PCR analysis.

Semi-quantitative PCR analysis of *hcn1*, *hcn2* and *gapdh* gene expression on mouse brain cDNA. Sizes of marker bands are indicated on the right. Primer pairs were tested for specificity and efficiency. Marker bands and their respective sizes are indicated on the right.

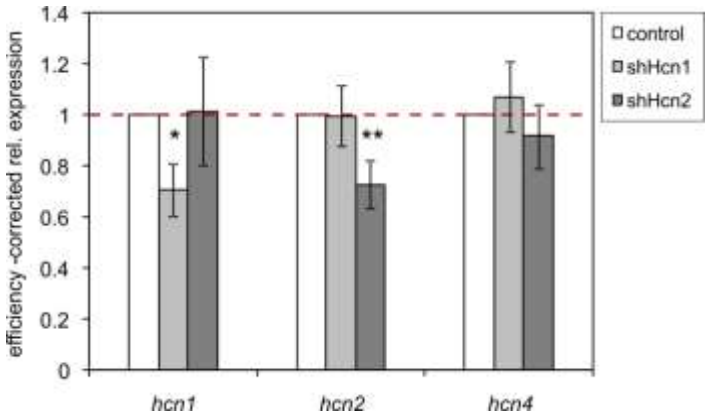

Fig. S2 Quantification of gene expression by real-time PCR.

Knockdown analyses for *hcn1*, *hcn2*, and *hcn4* in primary hippocampal neurons after 14 days in vitro are shown as the efficiency-corrected expression of *hcn* genes in relation to *gapdh*. Specificity and efficiency of knockdown was analyzed for *hcn1* (n=4) and *hcn2* (n=6) as well as *hcn4* (n=3) as an independent control gene and mean values are depicted for each target gene. Samples were treated for 12 d with rAAV9_CaMK2-eGFP_hU6-shHcn1, rAAV9_CaMK2-eGFP_hU6-shHcn1 or treated with vehicle as a control. Relative transcript expression of target genes was normalized to the vehicle-treated control. Error bars indicate s.e.m. and the level of significance is indicated (Student's *t* test: * $p< 0.03$; ** $p< 0.02$).